ARCHITECTURAL IMPLEMENTATION OF VEGETATED COVER FROM AGRICULTURE FOR RESTORING HUMAN THERMAL COMFORT AND MITIGATING THE URBAN HEAT ISLAND EFFECT IN ARID REGIONS

I.E. GAXIOLA[1], N.V. CHALFOUN[2] & C. MOELLER[2]
[1] Arid Lands Resource Sciences, The University of Arizona, USA.
[2] College of Architecture, Planning and Landscape Architecture, The University of Arizona, USA.

ABSTRACT

This investigation describes improved outdoor Human Thermal Comfort levels, based on the effects of integrating vegetated surfaces, such as those from Urban Agriculture systems, to architecture components of a building envelope within Tucson, Arizona, which can contribute on Urban Heat Island mitigation. Urban Agriculture comprises the integration of crop production with the built environment, it can contribute to improving buildings' performance, reducing air pollution, alleviating food scarcity, reducing stormwater runoff, decreasing fossil fuel use, and restoring Human Thermal Comfort. A methodology for outdoor Human Thermal Comfort assessment was applied. It involved the use of digital analysis of fish-eye lens photographs, and 'OUTDOOR', a computer software developed by Nader Chalfoun, Ph.D., at the University of Arizona, which is capable of calculating Human Thermal Comfort indices. Assumptions of this study include: access to water, soil, air, a building envelope, and the presence of vertical and horizontal arrangements of vegetated surfaces, produced in successfully developed Urban Agriculture systems around a selected building envelope in a hot-arid climate. Existing Human Thermal Comfort conditions were compared to those simulated with the integration of vegetated surfaces in order to evaluate the potential effects of Urban Agriculture, and to reach restored Human Thermal Comfort levels.

Keywords: fish-eye lens photograph, hemispherical photography, human thermal comfort, human view-factor, mean radiant temperature, urban agriculture, urban heat island.

1 INTRODUCTION

The built environment is one of the most intricate man-made systems. In view of this, attempting to achieve efficient use of resources and energy while adapting to climate conditions can help determine the physical characterization of a city. From the above, it can be stated that adequate models of human shelter and food production are required to optimally operate while dealing with complex environmental phenomena.

Among these phenomena, Urban Heat Islands (UHI) represent a consequence of intensified human activity, urban sprawl and arguably unwise employment of building materials. It is mainly driven by overconsumption of energy in urban cores and the building materials we use that store more heat compared to natural vegetated conditions. It is commonly characterized as the presence of different levels in temperature when comparing an urban development and its corresponding non-urban surrounding [1] (Fig. 1), and it tends to be stronger during night time [2].

Thermal energy radiated by building materials has a direct impact on Human Thermal Comfort (HTC). It is more difficult for the human body to maintain its optimal temperature level while receiving excessive heat from its surroundings in hot conditions where the air temperature is above the skin temperature and there is no mechanism to dissipate heat [3]. Herein, it is important to take careful consideration of the geometry of space [2], and thermal properties of materials (e.g. albedo, emissivity, specific heat, heat capacity, and surface

ISSN: 1755-7437 (paper format), ISSN: 1755-7445 (online), http://www.witpress.com/journals
DOI: 10.2495/DNE-V13-N4-373-383

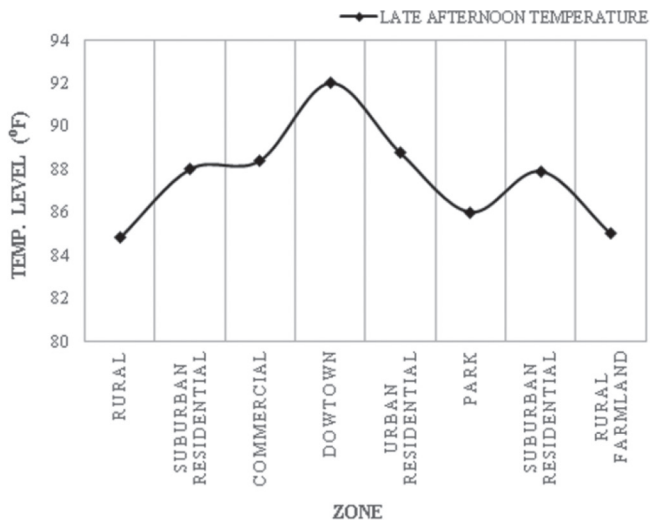

Figure 1: Sketch of urban heat island effect (Reproduced from http://ei.lehigh.edu/eli/luc/resources/uhi_profile.gif).

temperature), particularly in outdoor spaces. Smart use of building materials and, the implementation of green infrastructure can contribute to decreasing the impact of UHI [4].

Different green infrastructure systems which can be incorporated to the design of buildings, for example, green roofs, porous pavement, rain gardens, bioswales, planting trees and shrubs, etc. [5]. As a special mechanism for growing crops within the built environment [6], Urban Agriculture (UA) can be considered as an additional category within green infrastructure approaches. Different UA systems can be adopted, according to spatial conditions of the built environment, to effectively produce urban vegetation. For example, roof gardens, hydroponics, aquaponics, greenhouses, plant factories with artificial light, and remote skylighting.

Roof gardens involve the growing of plants on rooftops and, are very useful for rainwater harvesting. Hydroponics involve a recirculating water system to provide nutrients for plants and do not require soil: an inert mean for the plant to grow is provided. Aquaponics are based on hydroponics, with the difference that in aquaponics, plant nutrients are supplied by fish-generated waste, which is chemically processed by bacteria that plants metabolize to grow. Greenhouses comprise a confined surface area covered with a transparent-translucent material, operate using multiple systems (ventilation, refrigeration, irrigation, lighting, fertigation, etc.), and can be energy efficient. However, to build and operate an energy-efficient greenhouse requires a certain level of technical knowledge on controlled environment systems [7].

A plant factory with artificial light is an indoors-controlled environment system that supplies artificial light for plants to grow [8]. Remote skylighting combines fiber optics and a geometric mechanism to collect sunlight and channel it to a desired point using a concave dish oriented towards the sun, and a distributor dish on the other end of the system [9].

From the above, it can be stated that successful UA systems require access to solar radiation, space to grow (e.g. land, building components, such as facades), infrastructure, soil, water, institutional support, and participatory citizens [10], [11]. Its contribution lies partly on the fact that cities lack the means to become self-sufficient regarding food production

thus, UA implies a reduction in energy use on transportation of food, and an increase in the amount of vegetated cover [5], which could improve thermal conditions of the built environment. Increasing evapotranspiration through vegetated surfaces in the built environment contributes to decreasing latent heat, otherwise, a greater amount of energy ends up being available as sensible heat, which represent an increase in surface temperature levels and potentially a more intense UHI [12]. For example, approximately half of a building cooling loads can be reduced, if its thermal performance is mostly defined by the building envelope, and it is appropriately shaded using vegetation. The effect will be less for internal load dominated buildings, such as typical large offices, data centers, factories, or hospitals. For this purpose, plant species need to be properly selected and located considering climate and building shape [13].

Appropriate combination of water components and vegetation contributes to decreasing temperature levels in outdoor spaces [14]. Temperature levels of bodies of water tend to be lower compared with surrounding building materials, to the point of accounting for a difference between 2 and 6°C [12]. Additional benefits include the option to store rainwater for irrigating UA and contribute to sequestering stormwater runoff [5].

Coupling aquaculture and agriculture outdoors is an example of how UA systems can aid on cooling outdoor spaces, not only by transpiration and shade provided by plants, but also by using water for direct evaporative cooling thus, the effective combination of water features and urban agriculture can contribute on mitigating UHIs [12]. Assumptions considered for this study were: (1) Proposed vegetated cover was regarded as a product of successfully developed UA systems in a hot arid climate, (2) Access to water, soil, air, and a building envelope was provided, (3) For analysis purposes, proposed water features were considered as always filled with water.

2 OVERVIEW OF METHODOLOGY

Hemispherical Photograph Analysis (HPA) was applied to five selected locations at Inna E. Gittings building, located within the main campus of the University of Arizona in Tucson, AZ. The execution of HPA, based on Watson and Johnson's method [15], allowed to estimate human thermal comfort indices in outdoor spaces.

First, site locations are selected according to study-specific thermal circumstances. Subsequently, the percentage of Human View Factor (HVF) of materials affecting HTC is calculated for each location. HVF is useful to define the portion of radiant energy received by a person from a source surface, in relation to a particular location in space [16]. This step involves the use of two fish-eye lens photographs with a field of view of 180 degrees each. One photograph is taken aiming to the sky, and the second one pointing to the ground, in order to account for a sphere sample. The camera must be levelled, oriented to the north, and elevated 3 feet from the ground, if the analysis considers a person in standing position (Fig. 2). Photograph samples are scaled to fit a 6-inch diameter circumference. Samples are overlapped with a 6-inch diameter circular grid divided into 1000 equal units of 0.02827 in^2 each. The grid represents a polar diagram of HVF for an individual in standing position [15] (see Fig. 2).

Processing of samples, for accounting surface area of building materials, can be manual or automatic. The former requires printing the polar grid in a translucent material and overlapping it with the fish-eye photograph. Then, the amount of grid units per each material can be accounted and then multiplied by 0.02827. The automatic method is more accurate and less time consuming, it involves the use of computer software to filter and trace the perimeters or shapes of each defined material and, as a result of the process, surface areas of different materials can be automatically estimated.

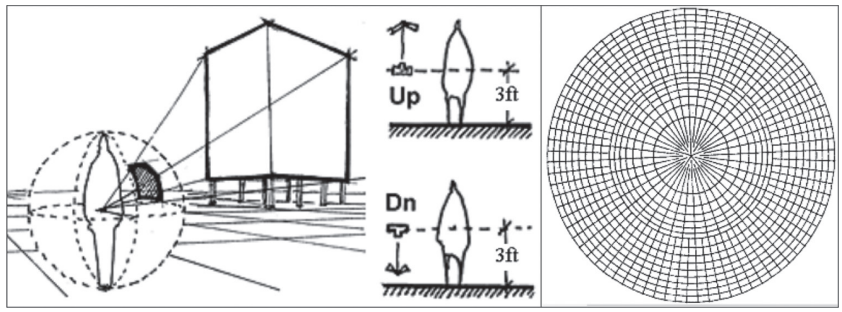

Figure 2: Scheme of radiant field affecting an individual. Left: representation of individual's view-factor and camera orientations for shooting fish-eye lens photographs *(Chalfoun, 2002*). Right: polar diagram of human view-factor for an individual in standing position (*Watson and Johnson, 1988*).

When complex shapes of vegetation show in photographs, effective extraction of surface area requires the combined use of vector- and pixel-based software. After estimating the surface area of each material within each sample, HVF is calculated using eqn (1).

$$HVF = \left(\frac{SAM}{GUA} \right) 0.0005 \tag{1}$$

Where:

- HVF = Human View Factor;
- SAM = Surface Area of Material (in^2) considering both hemispheres;
- GUA = Grid unit area, taken as 0.02827 in^2. It is a unit from a thousand in which a circular area with a diameter of 6 inches is divided, see right side of Fig. 2;
- 0.0005 = Correction factor of unity as a conservation of radiation leaving all surfaces that affect the two hemispheres of the human comfort spherical region.

Once the HVF has been calculated, meteorological and geographical data, as well as thermal properties of materials can be supplied to 'OUTDOOR' software. The data can be gathered on site, extracted from a Typical Meteorological Year (TMY) file, and from existing literature or official websites. An on-site survey of surface temperature of materials can be employed to provide a detailed profile of surface temperature variation throughout the day. Noncontact temperature measurements of close range targets can be made using an infrared thermometer.

An adequate temporal resolution aids on detecting trends in thermal comfort indices; hence, before employing 'OUTDOOR', a total amount of tests per day requires to be specified. For this study, six (one every four hours) were the selected amount of calculations. After estimating human thermal comfort indices in 'OUTDOOR', worst-case scenarios are identified then, improved spatial conditions can be proposed using a digital 3D model. Finally, fish-eye lens images generated from the digital 3D model are processed, and 'OUTDOOR' estimations are performed. This iterative process goes on until satisfactory HTC levels are reached.

3 HEMISPHERICAL PHOTOGRAPH ANALYSIS AND 'OUTDOOR' SOFTWARE

What follows are five steps describing HPA application to fish-eye photograph samples gathered at Ina E. Gittings Building, located within the Main Campus of the University of Arizona, in the hot-arid city of Tucson, AZ; and the use of 'OUTDOORS' for estimating HTC indices.

3.1 Site identification

Five outdoors locations were selected from Inna E. Gittings building, in the north-east region of the University of Arizona main campus (Fig. 3, center). Since the building dates from 1964, structural deficiencies could be a concern if heavy UA systems were to be attached to it. However, what made it suitable as a research case for an UA study were its large and simple walls, its strategic location within campus, presence of vegetation, and the access to water granted by existing infrastructure.

Criteria to select sampling locations consisted on identifying presence of vegetated surfaces, prevailing materials, geometry of space (particularly openness to the sky), and potential to integrate infrastructure of UA systems.

Location 1 is an uncovered esplanade with presence of vegetation on the north side, and neighboring an asphalt street on the south. Location 2 is an uncovered walkway with presence of vegetation, dirt, and high emissive materials. Location 3 is an uncovered courtyard with scarce vegetation and high emissive materials. Location 4 is a narrow, uncovered hall with no vegetation, flanked by high brick walls. Location 5 is a roof located on the south-west zone of the site. It has high reflectance and no vegetation (Fig. 3, center).

3.2 Gathering fish-eye lens photographs

Useful photographs were captured when uniform lighting conditions were present on building materials, particularly a few minutes after sunset [17]. A Nikon D610 Fx DSLR camera, with a SIGMA 8mm F4 circular image fish-eye lens attached, was mounted on a tripod, oriented to magnetic north, levelled, and the tip of the lens was set to a height of 3 feet for both, sky and ground samples (Fig. 4, left). Examples of useful photographs are: sample 02 (F-stop = f/16, exposure = 1/80 sec, and ISO = 6400), sample 03 (F-stop = f/11, exposure = 1/400 sec, and ISO = 6400), and sample 04 (F-stop = f/8, exposure = 1/1600 sec, and ISO = 6400), see right side of Fig. 4.

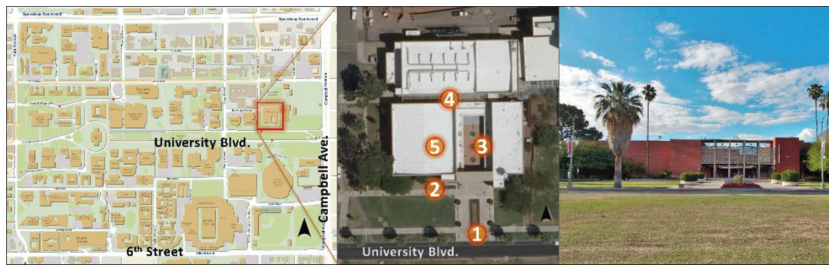

Figure 3: Study site. Left: aerial view of U of A main campus (*GIS MapTucson and U of A map*). Center: plan view of selected locations (*Google earth*). Right: south façade of case study building (*Gaxiola, 2016*).

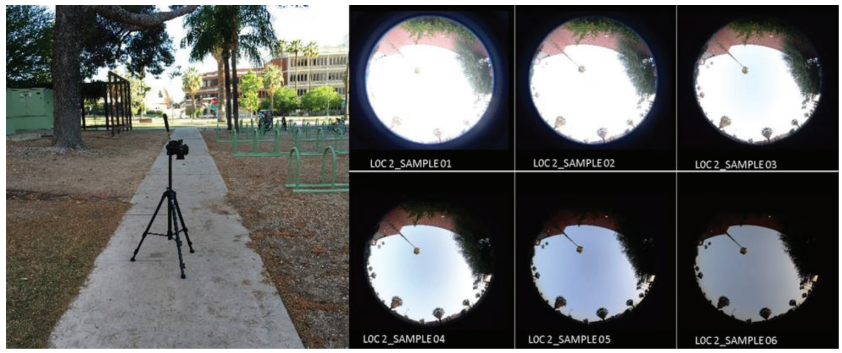

Figure 4: Fish-eye lens photograph samples. Left: camera set for a ground sample. Right: six samples aiming to the sky at location 2.

3.3 Digital analysis of fish-eye lens pictures

This phase was developed using AutoCAD, Photoshop, ImageJ, and the Photo editor from Microsoft. Two distinct cases were found while analyzing fish-eye pictures. The first had scarce or no vegetation shown in the pictures, the second case had abundant vegetation overlapping with surfaces of building materials.

The first step for accounting surface area was to scale each fish-eye picture in AutoCAD so that the useful circular area had a 6-inch diameter. After visually identifying materials, vectors were traced on their perimeters (Fig. 5, center). Then, vectors were set to layers, solid-color regions were generated and, if no vegetation was present, surface area was directly estimated in AutoCAD (Fig. 6, right).

For estimating surface area in pictures with abundant vegetation, the layer including all plant species was filtered using Photoshop, and then it was subtracted from the building material of interest and, after adding a 1-in^2 black square as scale reference, surface area was retrieved using particle analysis in 'ImageJ' (Fig. 7).

Once the surface area was calculated for each material in both fish-eye pictures of every location, HVF was calculated using eqn (1). Resulting HVF for each individual material was fed in 'OUTDOOR', in addition to meteorological and geographical data, adequate Clothing Insulation factor (CLO), Metabolic Rate values (MET), and thermal properties of materials gathered on site. For this study, a value of 0.5 for CLO, and 2.0 for MET were considered as applicable for users performing academic activities during summer in the main campus of the

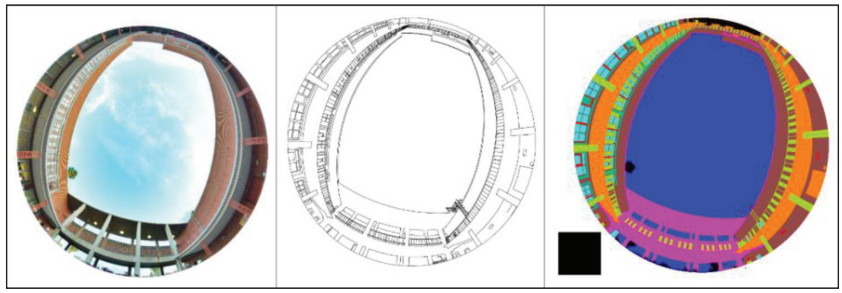

Figure 5: Sky photograph sample, location 3. Left: original photograph. Center: vectored sample. Right: Materials layered in color, the black square is the scale reference.

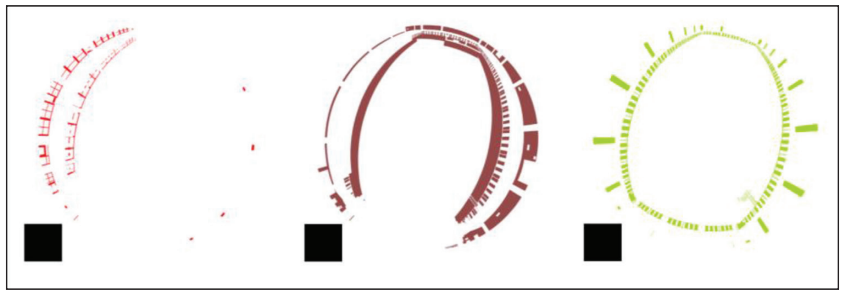

Figure 6: Three vectorised materials from location 03 after being processed in AutoCAD. Left: Aluminium. Center: Brick. Right: Iron.

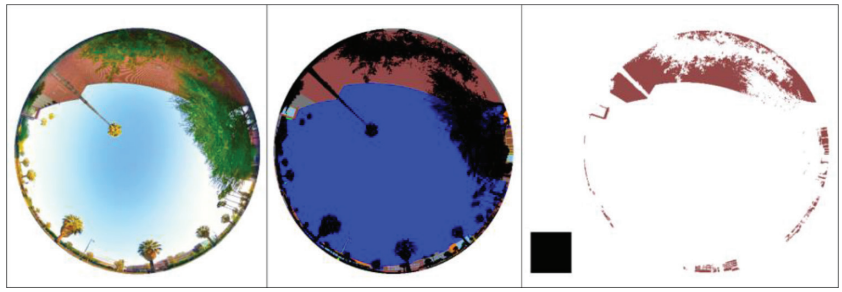

Figure 7: Sky fish-eye lens photograph, location 2. Left: original photograph. Center: vectorised materials. Right: final version of a sample material (brick) ready to be analysed in 'ImageJ'.

University of Arizona, in the hot-arid city of Tucson, AZ. Results from 'OUTDOOR' analyses were employed to detect trends in thermal conditions of the space in question, and worst case scenarios were identified.

3.4 Data Interpretation, balancing levels of thermal radiation

After performing 'OUTDOOR' estimations, location 03 (L03) was selected as the worst case scenario and; as suitable for UA implementation. Initial HVF on L03 showed highly radiating surfaces (Fig. 8). Considering a Predicted Mean Vote (PMV) range from −0.5 to +0.5 as comfortable [18], 'OUTDOOR' estimations on L03 at 8:00am, 12:00pm and, 4:00pm with 0% of shade, presented the highest uncomfortable PMV levels: 2.17, 2.75 and, 3.18, respectively.

'OUTDOOR' results aided on identifying dominant conditions of high PMV values: overexposure to radiation from brick, concrete, and open sky. Then, an alternative balanced HVF (Fig. 8) was proposed and used in 'OUTDOOR' with the scope of reaching a restored thermal comfort condition.

3.5 Digital modelling HTC restoration

After examining HTC indices using 'OUTDOOR', a digital 3D model of the building envelope was created using SketchUp, including landscape, urban furniture, and surrounding buildings (Fig. 9). Highly accurate fish-eye lens images were developed from the digital 3D

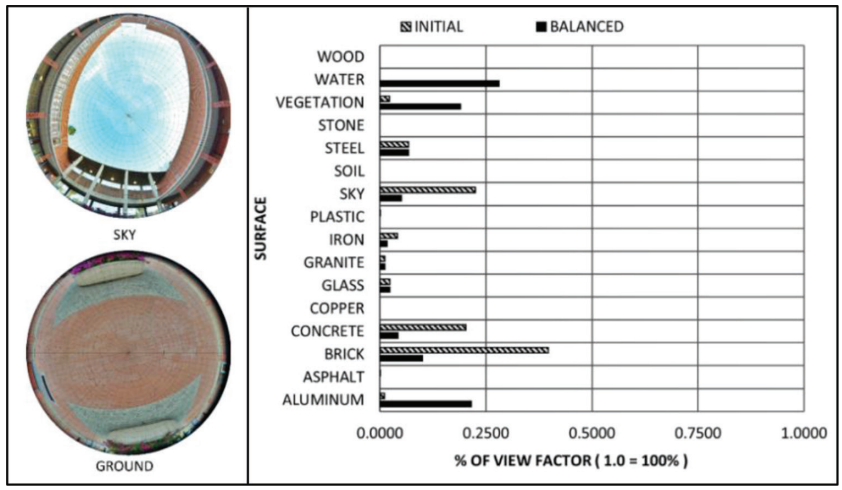

Figure 8. Left: fish-eye photographs of Location 03. Right: %VF values before and after balancing radiating surfaces.

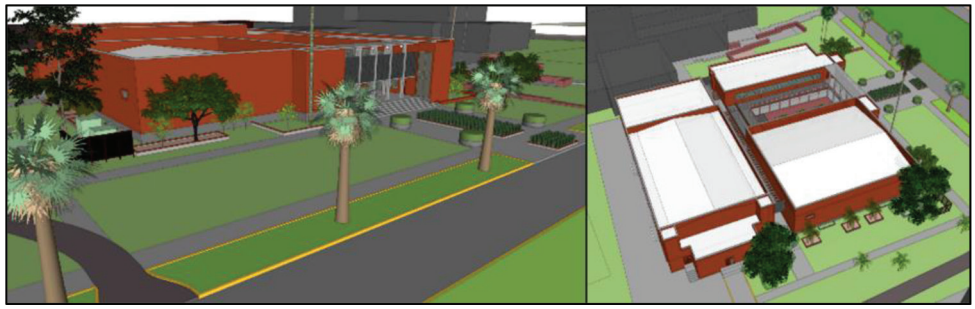

Figure 9: Existing conditions of the site. Digital 3D model created in SketchUp. Left: Southwest aerial perspective. Right: Northeast aerial perspective.

model using a rendering engine called POV-Ray: a fish-eye lens camera was configured and located in the digital 3D model on the same position as in the actual site (Fig. 10, center). Then, HVF was directly measured in 'ImageJ' using fish-eye rendered samples of isolated materials (see right side of Fig. 10).

This method allowed to execute faster 'OUTDOOR' estimations of environmentally retrofitted scenarios created in the digital 3D model. According to a climate analysis for the city of Tucson executed in Climate Consultant, in order to grant outdoor thermal comfort during critical hours (June 21st at 4 pm on Location 3 of the research case), selected strategies were: shading, vegetated cover, and water bodies. The combination of these strategies can improve HTC mainly through direct evaporative cooling, evapotranspiration, and shade [14], while also allowing to potentially regulate incident sunlight access for potential UA development.

In order to find the suitable HVF of every material, an iterative process was executed from 'OUTDOOR' back to the digital 3D model, and vice versa. Improvements were achieved by decreasing surface area of brick and concrete, adding vegetation, increasing shade, and incorporating a water body. The location and geometry of the spatial renovation was designed considering potential UA agriculture systems. As shown in Fig. 11, horizontal and vertical

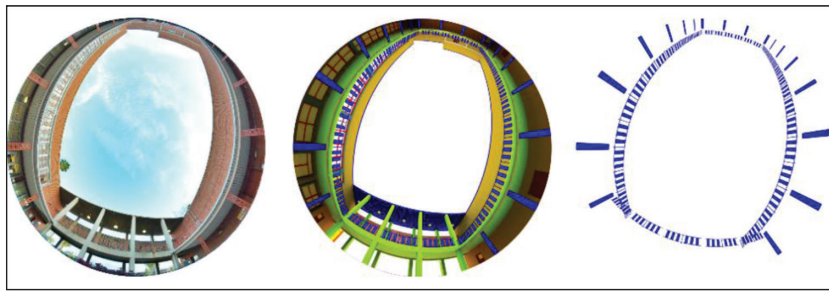

Figure 10: Comparison between a real fish-eye lens sample (left) and an image rendered in POV-Ray using a fish-eye camera on the same location (center). Fish-eye sample of a single material (right).

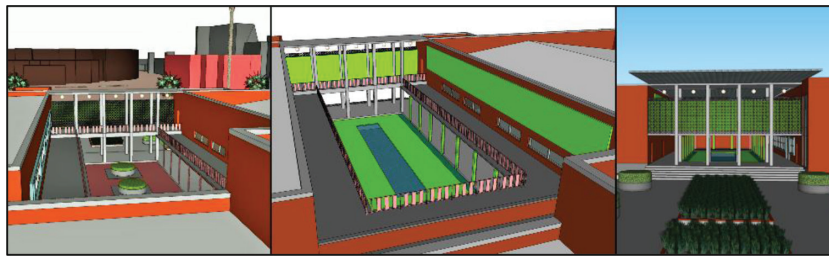

Figure 11: Perspectives of proposed improved conditions. Left: original building conditions. Center: Aerial view of courtyard with vegetated surfaces and central body of water. Right: south façade showing a horizontal aluminium shading structure.

planes in green represent vegetated surfaces, a body of water was proposed in the middle of the courtyard, and a louvered horizontal structure made out of aluminium was proposed on top of Location 03, in order to control solar radiation.

Noticeable improvements in HTC were found after implementing green infrastructure, considering the option of 100% shading conditions. At selected times when the building in question is operating (8:00, 12:00 and 16:00 hours), PMV levels decreased from 2.17, 2.75 and 3.18 to complying levels of -0.4, 0.5 and 0.5, respectively [18] (Fig. 12). MRT levels

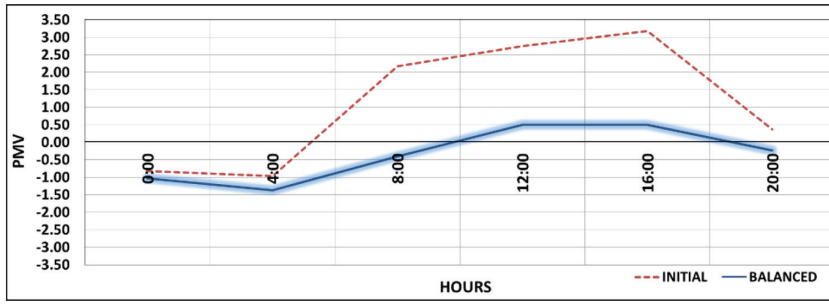

Figure 12: Line chart showing decrease on PMV levels after applying green infrastructure to the building envelope. The red dotted line represents PMV results in conditions with no shade. The blue line belongs to PMV values of improved conditions with full shade.

were reduced, for the hours mentioned above, from 130.4°F, 149.4°F and 170.8°F to 40.78°F, 60.41°F and 58.62°F, respectively. Effective Temperature (ET) levels of the final design proposal were reduced to 64.66°F, 74.80°F and, 74.72°F for 8:00, 12:00, and 16:00 hours, respectively.

4 CONCLUSIONS

Digital processing and generation of fish-eye lens photographs, aided by using 'OUTDOOR' software, allowed to analyze, simulate, and propose outdoor HTC conditions of an educational building located in the hot-arid city of Tucson, AZ. Simulations of a retrofitted outdoor space proposal, which incorporated strategic location of vegetated cover, a water feature, and shade, showed comfortable levels of PMV. By creating fish-eye lens images using a rendering engine, it can be stated that on site fish-eye samples are not completely necessary.

At building scale, the location and amount of surface materials is directly related to HTC. For example, the potential thermal impact/benefit of a surface material can increase as it is closer to human bodies. In addition to outdoor spaces being suitable for implementing urban agriculture, indoors implementation can be of use to reach better air quality, and psychological comfort.

Water bodies can be incorporated, and coupled with vegetated cover outdoors as direct evaporative cooling components, and as an irrigation resource for UA.

Thermal conditions in outdoor spaces can be optimized by regulating short- and long-wave radiation to provide HTC, with the additional benefit of crop production. Thus, excessive heat can be managed at urban scale by replicating and strategically placing improved microclimate outdoor thermal scenarios that include UA.

Future research avenues include determining a total amount of vegetated cover for decreasing the UHI effect in a given city, the use of drones for gathering fish-eye picture samples, and studying the thermal effect of individual plant species.

REFERENCES

[1] Cermak, J.E., Davenport, A.G., Plate, E.J. & Viegas, D.X. (eds), *Wind Climate in Cities* [Internet]. Springer Netherlands: Dordrecht, 1995 [cited 31 December, 2015]. Available from http://link.springer.com/10.1007/978-94-017-3686-2

[2] Oke, T.R., The energetic basis of the urban heat island. *Quarterly Journal of the Royal Meteorological Society*, **108(455)**, pp. 1–24, 1982.

[3] Moe, K., *Thermally Active Surfaces in Architecture*, p. 240, 1st edn., Princeton Architectural Press: New York, 2010.

[4] US EPA. Heat Island Cooling Strategies [Internet]. 2015 [cited 17 May, 2016]. Available from https://www.epa.gov/heat-islands/heat-island-cooling-strategies

[5] Daniels T. *The Environmental Planning Handbook for Sustainable Communities and Regions*, p. 548, 2nd edn., APA Planners Press: Chicago, 2014.

[6] Lupia, F. & Pulighe, G., Water use and urban agriculture: Estimation and water saving scenarios for residential kitchen gardens. *Agriculture and Agricultural Science Procedia*, **4**, pp. 50–58, 2015. https://doi.org/10.1016/j.aaspro.2015.03.007

[7] Philips, A., *Designing Urban Agriculture: A Complete Guide to the Planning, Design, Construction, Maintenance and Management of Edible Landscapes*, p. 288, 1st edn., Wiley: Hoboken, New Jersey, 2013.

[8] Toyoki Kozai. What PFAL means to urban agriculture. *Resource Magazine*, **20(2)**, p. 12, 2013.

[9] Drumm, P., The LowLine: How Do the Remote Skylights Work? [Internet]. Core77, 2012 [cited 5 May, 2016]. Available from: http://www.core77.com//posts/22088/The-LowLine-How-Do-the-Remote-Skylights-Work

[10] Jacobi, P., Drescher, A. & Amend, J., Urban Agriculture Justification and Planning Guidelines. Urban Vegetable Promotion Project [Internet], 2000 May [cited 9 April, 2018]; Available from https://d3n8a8pro7vhmx.cloudfront.net/erc/pages/46/attachments/original/1447203906/Urban_Agriculture_-_Justification_and_Planning_Guidelines.pdf?1447203906

[11] Angotti, T., Urban agriculture: long-term strategy or impossible dream?: Lessons from Prospect Farm in Brooklyn, New York. *Public Health*, **129(4)**, pp. 336–341, 1 April, 2015. https://doi.org/10.1016/j.puhe.2014.12.008

[12] Qiu, G., Li, H., Zhang, Q., Chen, W., Liang, X. & Li, X., Effects of evapotranspiration on mitigation of urban temperature by vegetation and urban agriculture. *Journal of Integrative Agriculture*, **12(8)**, pp. 1307–1315, 1 August, 2013. https://doi.org/10.1016/s2095-3119(13)60543-2

[13] Lechner, N., *Heating, Cooling, Lighting: Sustainable Design Methods for Architects*, p. 912, 4th edn., Wiley: Hoboken, New Jersey, 2015.

[14] Robitu, M., Musy, M., Inard, C. & Groleau, D., Modeling the influence of vegetation and water pond on urban microclimate. *Solar Energy*, **80(4)**, pp. 435–447, 1 April, 2006. https://doi.org/10.1016/j.solener.2005.06.015

[15] Watson, I.D. & Johnson, G.T., Estimating person view-factors from fish-eye lens photographs. *International Journal of Biometeorology*, **32(2)**, pp. 123–128, June 1988. https://doi.org/10.1007/bf01044905

[16] Chalfoun, N.V., Sustainable urban design and outdoor space analysis using MRT, and photography of scale models: A case study of the Rio Nuevo project in Tucson, Arizona, USA. In *PLEA* [Internet]. Toulouse, France, 2002 [cited 22 May, 2016]. Available from http://capla.arizona.edu/hed/docs/PleaToulouse.pdf

[17] Rich, P., *A Manual for Analysis of Hemispherical Canopy Photography. Los Alamos National Laboratory Report*. 1 January, 1989, LA-11733-M.

[18] Anderson, K., *Design Energy Simulation for Architects: Guide to 3D Graphics* [Internet], p. 272, Routledge: New York, Oxfordshire, England, 2014. Available from: https://www.amazon.com/Design-Energy-Simulation-Architects-Graphics/dp/041584066X/179-9162303-0525732?ie=UTF8&*Version*=1&*entries*=0